JACS
JOURNAL OF THE AMERICAN CHEMICAL SOCIETY

Article

Radical Hydroarylation of Functionalized Olefins and Mechanistic Investigation of Photocatalytic Pyridyl Radical Reactions

Ciaran P Seath, David B Vogt, Zihao Xu, Allyson J Boyington, and Nathan T. Jui

J. Am. Chem. Soc., **Just Accepted Manuscript** • DOI: 10.1021/jacs.8b10238 • Publication Date (Web): 24 Oct 2018

ACS Publications

is published by the American Chemical Society. 1155 Sixteenth Street N.W., Washington, DC 20036

Radical Hydroarylation of Functionalized Olefins and Mechanistic Investigation of Photocatalytic Pyridyl Radical Reactions

Ciaran P. Seath, David B. Vogt, Zihao Xu, Allyson J. Boyington and Nathan T. Jui*

Department of Chemistry and Winship Cancer Institute, Emory University, Atlanta, Georgia 30322

Supporting Information Placeholder

ABSTRACT: We report the photoredox alkylation of halopyridines using functionalized alkene and alkyne building blocks. Selective single-electron reduction of the halogenated pyridines provides the corresponding heteroaryl radicals, which undergo anti-Markovnikov addition to the alkene substrates. The system is shown to be mild and tolerant of a variety of alkene and alkyne subtypes. A combination of computational and experimental studies support a mechanism involving a proton-coupled electron transfer, followed by medium-dependent alkene addition and rapid hydrogen atom transfer mediated by a polarity-reversal catalyst.

Introduction

Functionalized pyridines are ubiquitous structural elements in bioactive small molecules that span a wide range of applications.[1] Accordingly, a number of powerful synthetic strategies have been developed to effectively access this heterocyclic family.[2] In addition to classical methods for pyridine construction using acyclic precursors,[3] diversification of pyridine units using transition-metal based cross-coupling[4] and C–H functionalization[5] strategies play key roles in modern drug discovery, as do nucleophilic aromatic substitution reactions.[6] Due, in part, to the orthogonal reactivity of radical intermediates to acidic (i.e. X–H) or Lewis-basic functional groups,[7] Minisci radical addition to pyridines remains a tremendously impactful retrosynthetic tool in complex pyridine synthesis.[8] However, the typical requirement for strong oxidants coupled with pronounced substrate-dependent regiocontrol limit the applicability of this strategy in many cases.[9]

Among others, we have utilized an alternative approach to complex (hetero)arene synthesis that operates through single electron reduction of halogenated aryl units to give rise to aryl radicals in a regiospecific manner.[10-11] In contrast to arenediazonium salts, this approach draws from a vast collection of stable, often commercially available substrates as radical precursors.[12] While arene activation in this manner requires the action of strong reductants, the introduction of photoredox catalysis has enabled the formation of highly reactive aryl radicals under mild conditions.[13] Our studies in this area have centered on the intermolecular reaction of pyridyl radicals with an array of olefin subtypes. Interestingly, we have developed conditions that enforce divergent reactivity profiles of these typically ambiphilic radicals, based solely on the reaction solvent (Figure 1). For example, in aqueous DMSO, pyridyl radicals selectively engage electron-poor alkenes through a radical conjugate addition (RCA) mechanism.[10a] However, the use of 2,2,2-trifluoroethanol (TFE) solvent enables highly-selective hydroarylation with simple, electron-neutral olefins.[11] Importantly, this protocol delivers the desired pyridyl products with complete regiocontrol with respect to both the heterocyclic and olefinic subunits (anti–Markovnikov addition), as a complement to recent

Figure 1. Catalytic intermolecular reactions of pyridyl radical intermediates

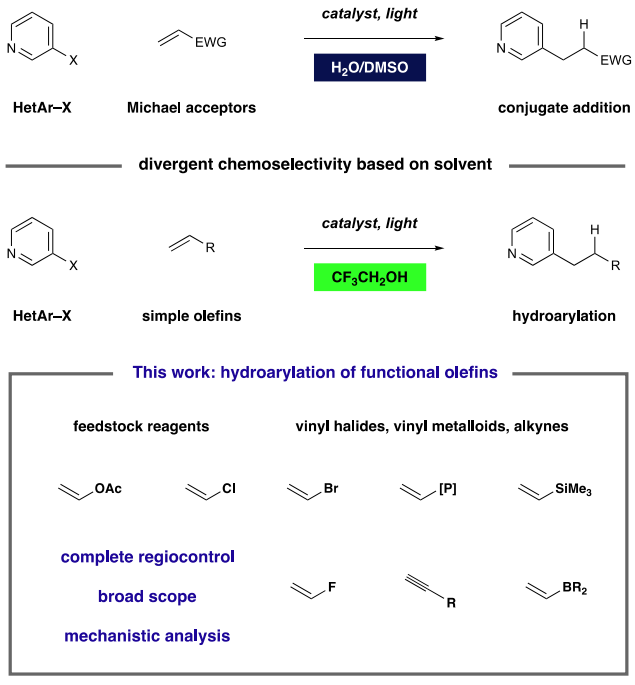

radical hydroarylation systems by Herzon[14] and Shenvi[15] (Markovnikov addition). Here, we describe the development of a system—based on this mechanistic blueprint—that allows for radical hydroarylation of a diverse collection of olefinic substrate classes. Many of these are shown for the first time as substrates under this synthetic disconnection, giving rise to densely functionalized alkylpyridines. In addition, we offer a mechanistic evaluation of these complementary pathways.

Results and Discussion

At the outset of this investigation, we treated the feedstock reagent vinyl acetate with 4-bromopyridine (**1**) under conditions that we recently described for anti-Markovnikov hydroarylation of aliphatic olefins.[11] More specifically, we employed the commercial iridium-based photoredox catalyst [Ir(ppy)$_2$dtbbpy]•PF$_6$ (1 mol%) and Hantzsch ester (HEH, 1.3 equiv) as a stoichiometric reductant using TFE as the reaction solvent. We found that irradiation of this mixture for 16 h with blue light furnished the desired pyridylethylacetate **2** in low yield (17%), and that the use of trifluoroethanol was crucial to product formation. However, significant amounts of oligomeric byproducts where pyridyl units coupled with multiple vinyl acetate equivalents (pyridine:olefin ratios of 1:2, 1:3, etc) were formed. We reasoned that increasing the rate of hydrogen atom transfer (HAT) to the nucleophilic α-oxy radical intermediate—resulting from radical addition to vinyl acetate—would preclude further olefin incorporation.[16] As such, we surveyed a number of electrophilic polarity reversal catalysts (Scheme 1).

Scheme 1. Anti-Markovnikov vinyl acetate hydroarylation using HAT catalysts[a]

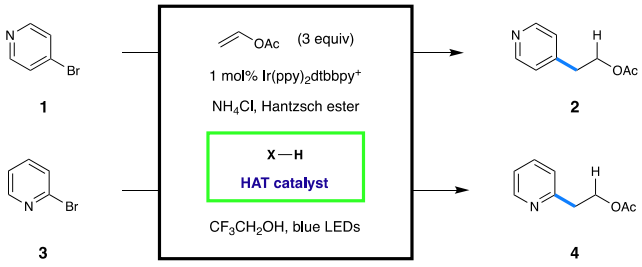

with HAT catalyst: (5 mol%)	none	NHPI	HOBt	CySH
yield of **2**[b]	17%	18%	22%	63%
yield of **4**	35%	52%	38%	65%

[a]Performed with Ir(ppy)$_2$(dtbbpy)•PF$_6$ (1 mol%), Hantzsch ester (1.3 equiv), halopyridine (1 equiv), vinyl acetate (3 equiv) in 2,2,2-trifluoroethanol (0.1 M) at 23 °C for 16 h, yields determined by ^{1}H NMR analysis. [b]4-bromopyridine hydrochloride used as substrate.

While the use of nitroxyl-based HAT catalysts NHPI[17] and HOBt[18] did not significantly alter reaction outcome, employment of cyclohexanethiol (5 mol% loading) resulted in significantly improved production of **2** (63% yield).[19] Here, a much cleaner reaction profile was observed where pyridine production (via radical hydrodehalogenation) was the major alternative pathway. The beneficial effect of thiol catalyst was also observed using the isomeric pyridyl radical precursor **3** as the limiting reagent, thus delivering the desired adduct **4** in 65% yield. A range of thiol HAT catalysts were surveyed, although no clear trend was observed between thiol electronics and reaction efficiency. Control reactions revealed that both photocatalyst and light were necessary for effective conversion and, in line with our previous results, acidic additives such as AcOH or NH$_4$Cl increased the yield. (see SI for details).

We then applied our optimized conditions to a variety of functional alkenes (containing heteroatom-substitution) that were absent from the current hydroarylation literature as well as common polymer feedstocks (Table 1).[20] Halogenated alkenes were particularly appealing, due to the broad utility of the products for further functionalization. Vinyl bromide was an effective coupling partner under the reaction conditions, affording alkyl bromide **6** in 78% yield, with no further reduction to the corresponding ethylpyridine. Exposure of the crude mixture to silica gel resulted in rapid, quantitative conversion to the corresponding vinyl pyridine, a product typically accessed through Stille cross-coupling with vinyl stannane.[21] 2-Chloropropene was similarly effective, providing secondary alkyl chloride **7** in 70% yield, again without undesired reduction of the resulting chloroalkane and elimination during purification was not observed in this case. The reaction conditions were also tolerant of alkenyl fluorides, producing alkyl fluoride **8** in good yield. Robust methods for the synthesis of alkyl fluorides are highly prized, particularly where S$_N$2-type approaches are competitive with elimination by-products.[22]

In a complimentary process to the recently described work of Aggarwal,[23] alkenyl boronic esters also underwent the reaction smoothly under the reaction conditions. Homobenzylic alkyl boronic ester **9** was effectively synthesized through this method (58%), without any undesired protodeboronation or oxidation. Alkenes substituted with main group elements were also readily incorporated, despite relatively scarce examples of the hydroarylation of these moieties and a dearth of knowledge around the reactivity of the resulting α-heteroatomic radicals.[24] Alkenes substituted with Si, S, and P were all tolerated, delivering **10**, **11**, and **12** in good yields (41-68%). We envision this method to be applicable towards the synthesis of novel bidentate P, N or S, N ligands that are non-trivial to access through other methods.[25]

Table 1. Anti-Markovnikov hydroarylation with pyridyl radicals: Scope of the functionalized olefin[a]

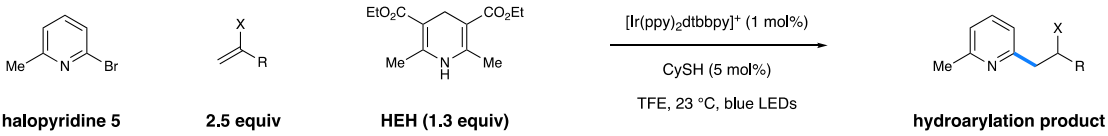

halopyridine 5 | 2.5 equiv | HEH (1.3 equiv) | hydroarylation product

olefin	product	compound #: yield	olefin	product	compound #: yield
	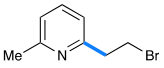	**6**: 78%		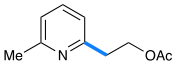	**13**: 57%
	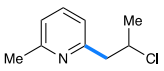	**7**: 70%		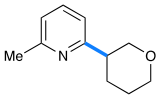	**14**: 72%
	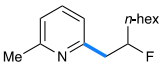	**8**: 65%[b]		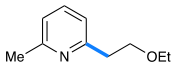	**15**: 62%
	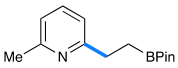	**9**: 58%[c]		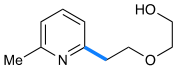	**16**: 72%
	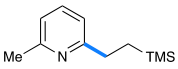	**10**: 68%		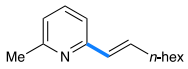	**17**: 75%, 1:1 (E:Z)
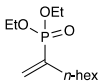	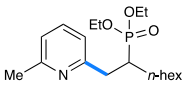	**11**: 41%[b]		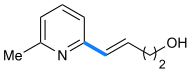	**18**: 83%, 1:1 (E:Z)
	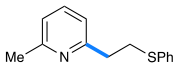	**12**: 52%		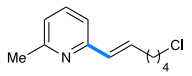	**19**: 66%, 1:1 (E:Z)

[a]Isolated yields. Performed with $[Ir(ppy)_2dtbbpy]•PF_6$ (1 mol%), Hantzsch ester (1.3 mmol), 2-bromo-6-methylpyridine (1 mmol), alkene (3 mmol) and CySH (5 mol%) in 2,2,2-trifluoroethanol (0.1 M) at 23 °C for 16 h. [b]Reaction performed on 0.1 mmol scale. [c]Reaction performed on 0.25 mmol scale.

The polymer feedstocks vinyl acetate and ethyl vinyl ether both combined with bromopyridine **5** in good yields (57% and 62% yield, respectively) where the remainder of the mass balance was hydrodehalogenated **5**, and not higher order oligomers. Alkyl enol ethers smoothly participated in the reaction to give **14** and **16** both in 72% isolated yield. In addition to heteroatom-substituted alkenes, a number of alkynes were smoothly converted by this system to provide the corresponding vinyl pyridines **17**–**19** as 1:1 mixtures of geometrical isomers (66%–83% yield). In particular, these transformations were unaffected by unprotected alcohols and primary alkyl chlorides. This method provides an alternative to classical Mizoroki-Heck chemistry, which is typically intolerant of such sensitive functionality.[26]

We next explored the scope of the halopyridine component using isopropenyl acetate as the olefinic coupling partner (as indicated in Table 2). The conditions were tolerant of alkyl substituents on the radical precursor (**20**, **24**–**25**), in addition to other electron donating groups including alkoxy **23** and carbamate functions **27,** with only minor deviations in yield (42–57%). Alkyne-containing pyridine **30** could also be synthesized under the reaction conditions (26%), providing exclusive chemoselectivity for alkene addition, leaving a useful functional handle for further manipulation. Fused heterocycles were likewise tolerated, pyrrolopyrimidine

Table 2. Scope of the halogenated pyridine[a]

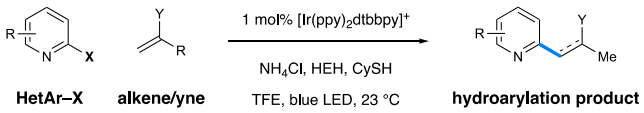

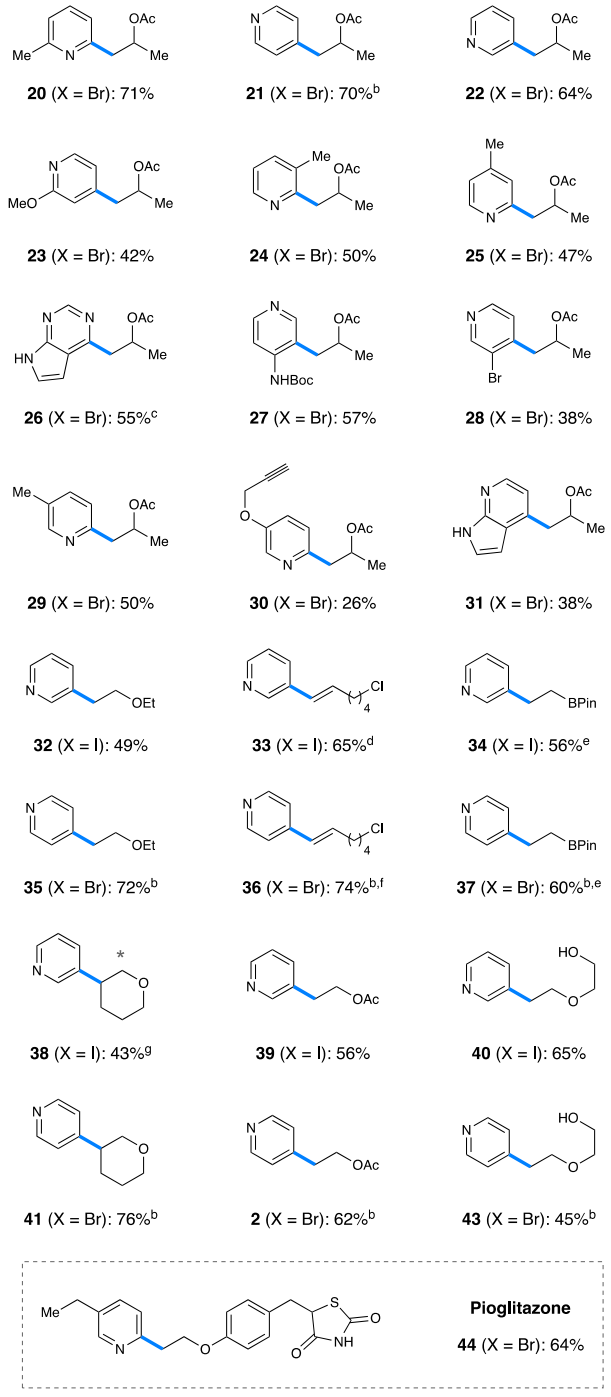

[a]Isolated yields, reactions were conducted as in Table 1. [b]4-Bromopyridine•HCl was used as starting material. [c]Reaction performed on 0.5 mmol scale. [d]Formed as a (1.7:1) mixture of olefin isomers. [e]Reaction performed on 0.25 mmol scale. [f]Formed as a (3:1) mixture of olefin isomers. [g]Isolated as a 1.2:1 mixture of regioisomers, grey asterisk indicates connectivity of the minor regioisomer.

26 and azaindole **31** being formed in moderate yields (38–55%). Moreover, 3,4-dibromopyridine underwent chemoselective reaction at the more electron-poor 4-position to provide alkylated bromopyridine **28** without subsequent reductive dehalogenation (38%). Here, radical anion fragmentation occurs selectivity through cleavage of the weaker C–Br bond (at the 4-position), and 3-bromopyridine comprised the mass balance (formed via hydrodebromination). To further illustrate the generality of the process for all pyridine regioisomers, a representative portion of the alkene scope were coupled to 3- and 4-halopyridines (Table 2, **32**–**42**). To further demonstrate the scope of the alkene-coupling partner, the anti-diabetic Pioglitazone[27] was prepared in a short synthetic sequence (Table 2, **43**, 64%) that utilizes an aryl vinyl ether as olefinic partner. The unique disconnection afforded by this hydroarylation protocol allows for a highly modular synthesis, which would be appealing for early stage discovery programs.[28]

This photoredox process was amenable to gram-scale synthesis without erosion of isolated yield (71 vs 76%). Compound **20** was synthesized on a 10 mmol scale without any specialized equipment using only 0.1 mol% Ir catalyst (Figure 2). It has been well demonstrated that scale up of photocatalytic processes can be limited by light penetration;[29] a common solution to this issue is the use of continuous flow methods,[30] which have facilitated the large scale production of active pharmaceutical ingredients.[31] To demonstrate that our method is amenable to such scale up procedures, we performed the reaction in a custom-built flow reactor. Using a plug-flow regime with a residence time of 20 minutes the alkylated product was formed in 75% yield, corresponding to a continuous flow production of 4.5 mmol/h. Further optimization of the flow reactor setup is ongoing within our laboratory.

Figure 2. Enol acetate hydroarylation on gram scale

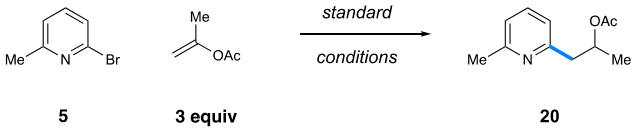

10 mmol scale in batch (16 h):	in a flow reactor (t_r = 20 min)
76% yield (1.5 g)	4.5 mmol/hour

Mechanistic Investigation

Having established the utility of pyridyl radical intermediates in hydroarylation processes of functional olefins, we were interested in gaining a deeper mechanistic understanding of this system. Of particular interest were the following two elements: (i) reductive

activation of halopyridine substrates is efficient even in cases where SET would appear to be endergonic (as indicated by thermodynamic reduction potentials), and (ii) pyridyl radical

Figure 3. Mechanistic Proposal: Solvent dictated nature of pyridyl radical, imparting divergent chemoselectivity

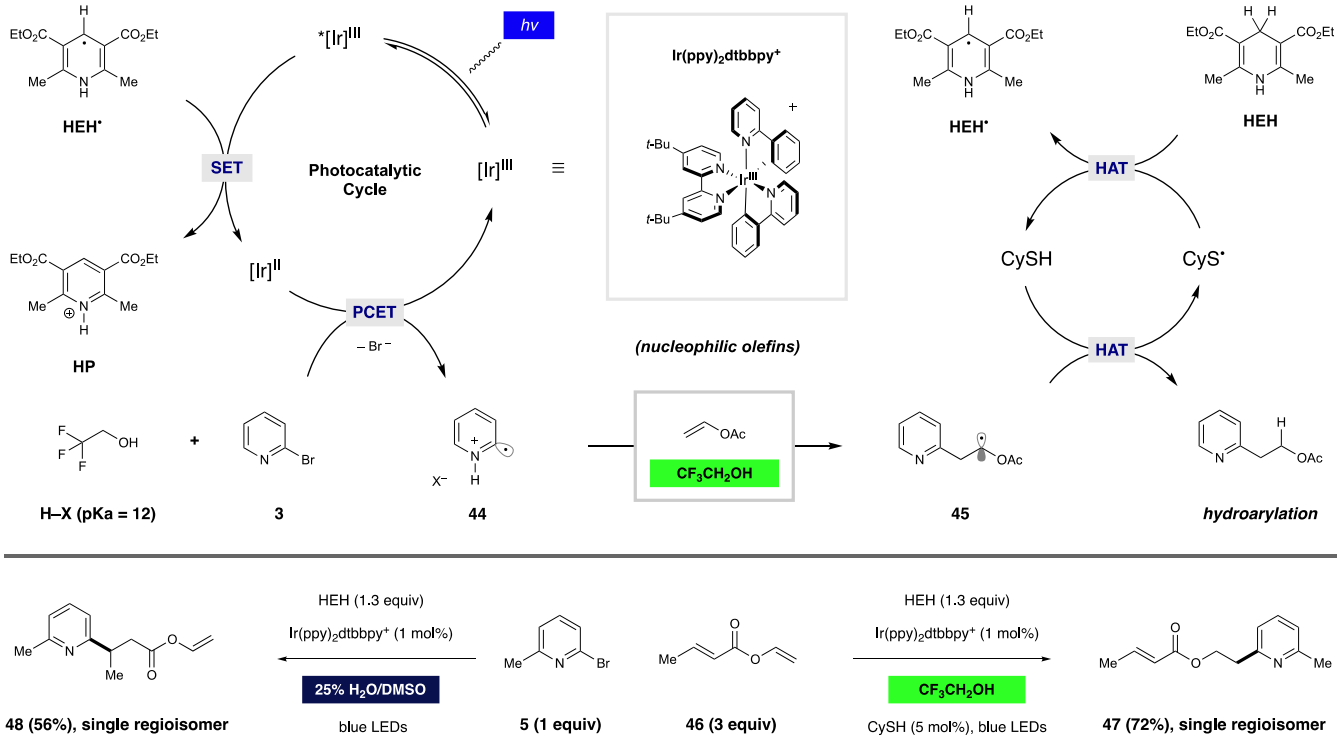

species display remarkable chemoselectivity for different olefin types depending on the reaction solvent.

Shown in Figure 3 is a proposed mechanistic scenario for the dual catalytic hydroarylation process that is introduced above. Specifically, reductive quenching of the photoexcited iridium catalyst (*[Ir]^{III}) would give rise to the reducing [Ir]^{II} species ($E_{1/2}^{0}$ = –1.51 V vs. SCE). This mechanism would likely be initiated by oxidation of a sacrificial amount of HEH, as supported by Stern-Volmer quenching studies in agreement with previous studies by Knowles.[32] Reduction of the bromopyridine substrate **3** via proton-coupled electron transfer (involving TFE as proton source), followed by rapid mesolytic cleavage would provide protonated pyridine radical **44** and an equivalent of bromide. Regioselective radical addition to the terminal carbon of vinyl acetate (like other nucleophilic olefins) would furnish radical species **45** that would undergo polarity-matched HAT from the thiol catalyst, concurrently producing the hydroarylation product and thiyl species. Regeneration of the HAT catalyst with HEH would deliver the corresponding dihydropyridine radical (HEH•), a mild reductant that would close the photoredox catalytic cycle delivering the corresponding pyridinium (HP).

Key to this electrophilic radical reactivity is the notorious hydrogen-bond donating (but poorly hydrogen-bond accepting) solvent TFE.[33] Indeed, when the diene compound vinylcrotonate **46** was reacted in trifluoroethanol, the pyridyl radical derived from bromopyridine **5** engaged the nucleophilic alkene, giving rise to hydroarylation product **47** as a single regioisomer (72% yield). In contrast, activation of the same radical precursor with the same catalyst but in aqueous DMSO as solvent (25% (v/v) H_2O/DMSO) resulted in exclusive radical conjugate addition to the Michael acceptor, affording **48** as a single regioisomer (56% yield). Regiochemical analysis in these experiments was conducted by GC and, in both cases, <1% of the alternate regioisomer was observed. Here, picoline production was the major alternative pathway. These results, completely consistent with a previously reported set of competition experiments, indicate that pyridyl radical addition to olefins operates through different reactive intermediates, as dictated by solvent.[11] Further evaluation of these scenarios is presented in the following sections.

Proton-coupled electron transfer (PCET)

As indicated above, we propose that pyridyl radical formation occurs primarily through a reductive quenching pathway of the iridium photocatalyst. However, analysis of the salient reduction potentials in this system is complicated. Accurate measurement of the reduction potential of halogenated pyridines remains a challenge because fragmentation of the resulting radical anions is rapid and pyridyl radicals readily undergo reduction to the corresponding anions. However, the reduction potential of 2-bromopyridine has been reported to be between –1.80[34] and –2.29 V[35] vs. SCE, which is significantly beyond the reducing ability of the Ir-catalyst

($E_{1/2}^0$ = –1.51 V vs. SCE). Although protonation of the halopyridine substrate would significantly decrease reduction potential ($E^0_{1/2}$ = –1.10 V), a cursory analysis of pK_a values of TFE (pK_a = 12 in DMSO) and 2-

Scheme 2. Proposed Mechanism of Reduction: PCET

(A) Calculated reduction potentials of pertinent mechanistic components

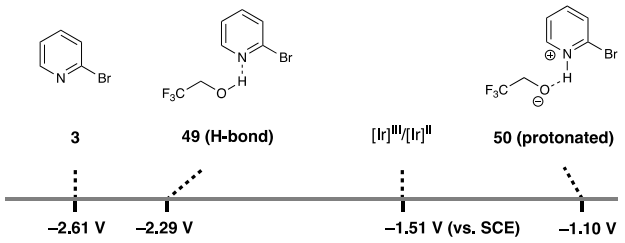

(B) Energetic consequences of bromopyridine (**3**) / TFE interaction

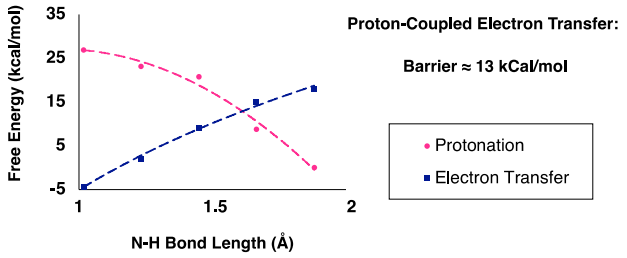

[a]DFT calculations performed at the uB3LYP level of theory using 6-311+G (d,p) CPCM = DMSO.

bromopyridinium (pK_a = 0.5 in DMSO) does not support formation of a discrete pyridinium salt. Thus, we reason that reductive activation of pyridine substrates in TFE occurs through a proton-coupled electron transfer (PCET) mechanism.[36]

The effect of pyridine protonation on the energetics of electron transfer has been well studied, particularly within the context of CO_2 reduction.[37] However, reports detailing the exact impact of protonation on pyridine reduction potential remain disparate. Because the complications associated with halopyridine reduction potential measurements (*vide supra*) are compounded by the fact that TFE has a narrow usable electrochemical window, we turned to DFT calculations to further interrogate this step (Scheme 2A). Using the uB3LYP level of theory, the reduction potential of 2-bromopyridine was calculated to be –2.61 V vs. SCE,[38] as were the potentials of H-bonded substrate **49** ($E_{1/2}^0$ = –2.29 V vs. SCE; N–H–O bond length 2 Å) and fully protonated substrate **50** ($E_{1/2}^0$ –1.1 V vs. SCE; 1.1 Å bond length). Indeed, the measured reduction potential of the $[Ir]^{II}$ catalytic species ($E_{1/2}^0$ = –1.51 V. vs. SCE) lies squarely between these values.[13] As shown in Scheme 2B, protonation of the neutral species with TFE is endergonic by 27 kcal/mol but is thermo-neutral after reduction. Similarly, reduction of bromopyridine at 2 Å is endergonic by 18.1 kcal/mol but exergonic by 9.4 kcal/mol after protonation. The lowest energetic barrier (where both lines converge) was calculated to be 13 kcal/mol at a N–H bond length of 1.55 Å, a reasonable energetic barrier for the proposed PCET event. An endergonic electron transfer of this is type is feasible from a ground state reductant based on the highly exergonic heterolytic cleavage event that occurs immediately post reduction (i.e. Curtin-Hammett principle). While this principle could account for a decoupled protonation/electron transfer sequence, we posit that a concerted mechanism is operative.

Chemoselective C–C bond-formation

Among the most interesting features of this pyridyl radical-based strategy is the highly-pronounced chemoselectivity that is imparted by the chosen reaction solvent. Shown in Scheme 3 are two electronically diverse olefins, along with the optimal reaction solvent for their intermolecular coupling with pyridyl radicals. Because high chemoselectivity for either electron-rich or -poor olefins has been observed (vide supra), we hypothesize that these complementary systems differ in the identity of the pertinent pyridyl radical species. More specifically, we propose that protonated, electrophilic radical species (e.g. **44**) are active in TFE, while proton dissociation in polar, H-bond accepting solvents favours neutral, nucleophilc aryl radicals (e.g. **51**).[39]

As an excellent H-bond donor and a weak H-bond acceptor, TFE has the ability to form strong H-bonding networks that effectively stabilize anions or protonate very weak bases.[33] As a result, the use of TFE as reaction solvent has led to divergent selectivity profiles in other systems that are reminiscent of our findings.[33] To investigate the relevance of this solvent property in our systems, we attempted to overturn observed pyridyl radical chemoselectivity through a series of competition experiments. As indicated in Scheme 3, treatment of **5** with both the electron-rich propenyl acetate and electron-poor dimethylethylidene malonate (3 equiv each) under standard conditions in TFE led to exclusive production of **20**. However, addition of various amounts of water was accompanied by increasingly significant formation of the radical conjugate addition product **52**. With 150 equiv H_2O, the two products were formed in nearly equal amounts, presumably resulting from increased dissociation of proton from the pyridyl radical species by the H-bond acceptor H_2O.[40] Addition of acids to the same mixtures in DMSO did not have an impact on chemoselectivity, which is also consistent with the suggestion that protons are highly dissociated from the pyridyl radical species in polar (aqueous) solvent.

An alternative set of reactive intermediates that could potentially account for the observed solvent-based complementary selectivity of this method could arise from differential rates of radical anion fragmentation, depending on solvent. In this scenario, an α-bromo, α-amino radical (resulting directly from PCET) would undergo C–C bond-formation prior to bromide

dissociation, presumably as an intermediate in radical conjugate addition (i.e. aq. DMSO). Indeed, Weaver has proposed that rate of radical anion fragmentation is responsible for altered selectivity in reductive photoredox

Scheme 3. Proposal for Observed Solvent-Dependent Chemoselectivity of Pyridyl Radicals

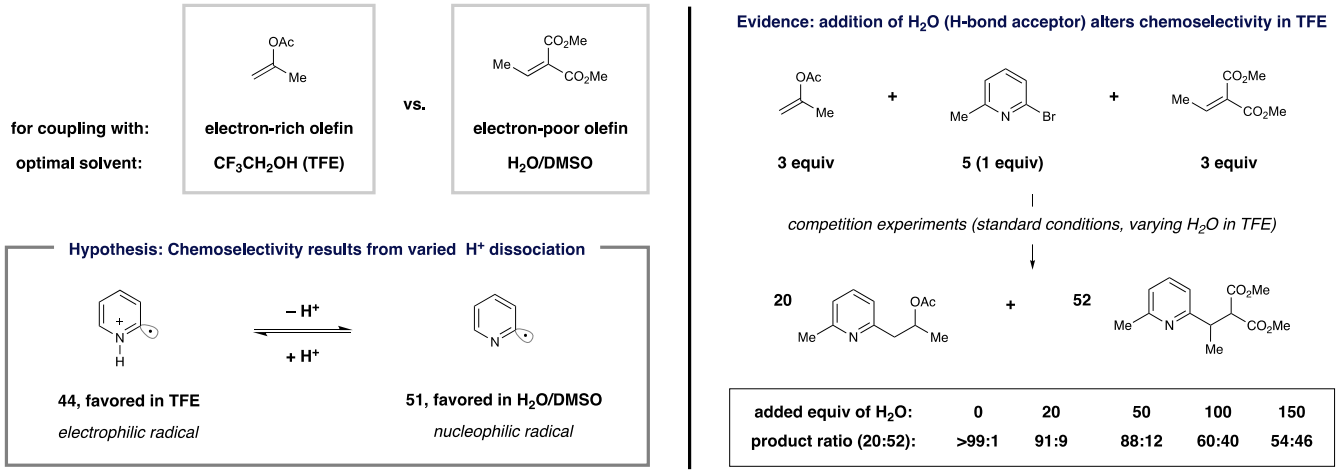

[a]Performed with $Ir(ppy)_2(dtbbpy)•PF_6$ (1 mol%), Hantzsch ester (1.3 equiv), 2-bromo-6-methylpyridine (1 equiv), dimethylalkylidine malonate (3 equiv), isopropenyl acetate (3 equiv) in 2,2,2-trifluoroethanol (0.1 M) at 23 °C for 16 h.

processes of 2-haloazoles (where differential reactivity resulted from different halogens).[41] Along the same lines, it has been shown that the rate of 2-halopyridine (2-X-pyr) radical anion fragmentation decreases significantly in the series X = I > Br > Cl >>F.[35a] While the fluoropyridine-based radical anion persists long enough to observe reversible redox by CV, bromopyridine radical anion fragmentation is exceedingly rapid, as measured by Savéant and others.[42] Solvent polarity has also been shown to alter fragmentation rate to a lesser extent, but unimolecular fragmentation rates remain significantly higher than the relevant bimolecular addition rates for aryl radical addition to olefins.[43]

Radical termination after alkene addition

During our investigations into addition of pyridyl radicals to olefins, we have observed different radical termination mechanisms that are highly dependent on the employed alkene subtype. While different reaction modes often lead to identical outcomes (e.g. Giese termination via HAT[44] or a reduction/enolate protonation sequence[45]), they could be expected to have discrete implications for photocatalyst turnover or, more importantly, the structural nature of the product. Using combinations of deuterium-labelled HEH and solvents, we have shown that dehydroalanine-derived **53** undergoes essentially exclusive reduction and enolate protonation to give the desired amino acid products.[10b] In contrast, radicals **54** and **55**, receive α-protons or deuterons primarily from HEH, indicating HAT as the primary termination events (>80% incorporation of the label from HEH, rather than solvent).[10a,11] When coupling to more nucleophilic vinyl heteroatoms is considered, both oxidation and HAT processes of the intermediate radical (e.g. **56**, derived from vinyl acetate) are relevant as they would likely be product determining. For example, in a method described by Buchwald, a similar α-oxy radical, generated from Meerwein addition to an enol acetate, is efficiently

Figure 4. Mechanisms of Radical Termination

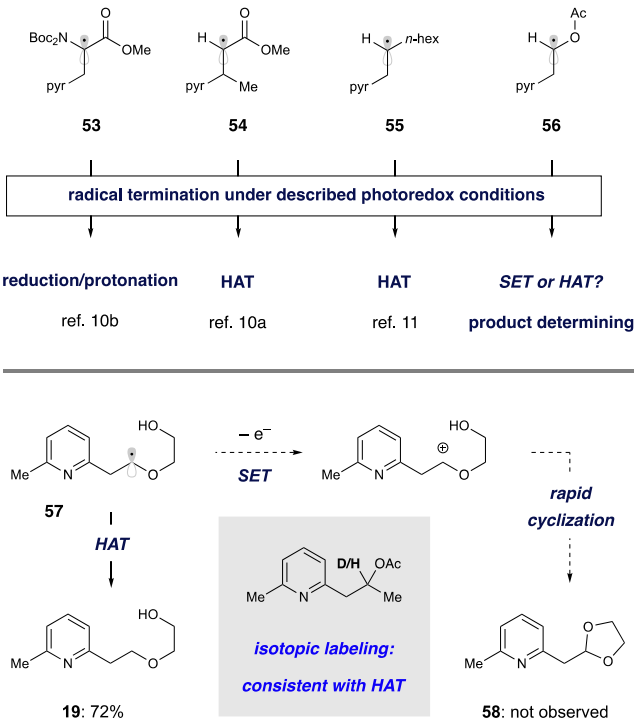

oxidized by ferrocinium to provide an aldehyde product.[46] However, the conditions that are introduced here appear to enforce termination via HAT, even though single electron oxidation of **56** would be facile ($E_{1/2}^0$ = 0.21 V vs. SCE).

Evidence for product formation via terminal HAT is offered in Figure 4, where both potentially competing

pathways involving radical intermediate **57** are illustrated. Work by Moeller,[47] and Horner and Newcomb[48] indicates that oxidation to the corresponding cation would be followed by exceedingly rapid cyclization to dioxolane **58**. However, hydroarylation product **19** was delivered in 72% yield, without any indication of **58** by NMR or GCMS analysis. Further, isotopic labelling experiments involving deuterated HEH and/or solvent were consistent with this proposal (see SI for details). The discrepancy between these results and the system reported by Buchwald[46] arises from effective concentration of the putative oxidant; 10 mol% Cp_2Fe^+ (generated through highly exergonic reduction of arenediazonium salts) vs minute concentration of photooxidant.

Alternative redox pathways

Although the mechanistic analyses that we present are consistent with experimental data, the observed results likely arise from an ensemble of related mechanistic pathways. For example, the proposed role of the stroichiometric reductant (HEH) is highly consistent with previous reports, facilitating product formation through sequential HAT and SET steps. However, the order of these events is experimentally ambiguous, as HEH consumption via the same steps in reverse order (SET then HAT) would reasonably lead to the same experimental results.

To further evaluate the validity of the proposed photoredox pathway, we conducted a series of temporal studies. Under these conditions, propenyl acetate hydroarylation (to give **20**) exhibited zero order kinetics (with respect to starting materials and catalyst) in a manner that was highly dependent on the light source,[49] as shown in Figure 5. In conjunction with the finding that the benchmark reaction reached completion within 10 min, these results led us to question the degree of radical chain character of this processes.[50] However, the relatively low quantum yield (Φ = 0.31) of this process indicates that photosensitized processes are dominant. Control experiments showed that formation of **20** can occur in the absence of the iridium catalyst, but the reaction rate is considerably slower (~10% yield after 16 h vs. 72% yield after 10 min, see supporting information for details). We suggest that the catalyst–free reaction arises from the HEH excited state reducing the halopyridine.[51] Charge transfer complexes between HEH and bromopyridine were not observed in either the ground state via ^{1}H NMR analysis or the excited state via UV/Vis spectroscopy (See SI for further details). Moreover, alteration of the catalyst properties had a noticeable impact on overall reaction efficiency (see SI for full details).[50] Taken in aggregate, these findings implicate the outlined catalytic manifold as the major contributor to product formation in this system.[50]

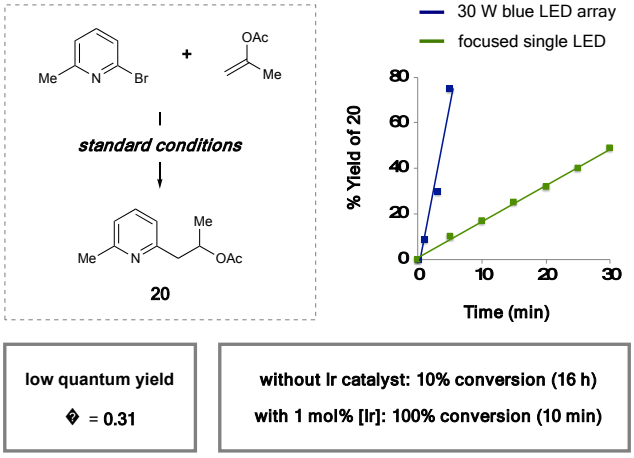

Figure 5. Temporal Evaluation of Reaction Profile

Conclusions

In summary, a general and efficient method for the hydroarylation of electron rich olefins has been developed. Addition of a thiol polarity-reversal catalyst promotes a rapid intermolecular HAT step that prevents side reactions such as olefin polymerization and single electron oxidation to provide the anti-Markovnikov products exclusively. Investigation of the reaction mechanism revealed a solvent dependent mechanistic divergence. Use of the highly coordinating solvent TFE, leads to a protonated, electrophilic pyridyl radical which is polarity matched for alkene addition with electron rich olefins. Use of a H-bond accepting medium such as $DMSO_{(aq)}$ leads to a dissociated, neutral pyridyl radical that is polarity matched for electron-poor olefins. We believe these data will provide a greater rationale for chemistries utilizing heteroaryl radicals and expand the scope and understanding of related radical-olefin couplings.

ASSOCIATED CONTENT

Supporting Information.

Experimental procedures and spectral data are available free of charge on the ACS Publications website.

AUTHOR INFORMATION

Corresponding Author

njui@emory.edu

Notes

The authors declare no competing financial interests.

ACKNOWLEDGMENT

This project was supported by funds from the National Institutes of Health (R01 GM129495), and NMR spectra were obtained under the support of the National Science Foundation (CHE-1531620). The authors would like to thank Savannah Post (Emory) for preliminary experiments, Professors R. Brian Dyer and Tianquan Lian (Emory) for generous access to instrumentation, and Professor Zachary Wickens (University of Wisconsin) for helpful discussions.

REFERENCES

(1) (a) Guan, A.-Y.; Liu, C.-L.; Sun, X.-F.; Xie, Y.; Wang M.-A. Discovery of pyridine-based agrochemicals by using intermediate derivatization methods. *Bioorg. Med. Chem.* **2016**, *24*, 342–353. (b) Vitaku, E.; Smith, D. T.; Njardarson, J. T. Analysis of the Structural Diversity, Substitution Patterns, and Frequency of Nitrogen Heterocycles among U.S. FDA Approved Pharmaceuticals. *J. Med. Chem.* **2014**, *57*, 10257–10274. (c) Bakhite, E. A.; Abd-Ella, A. A.; El-Sayed, M. E. A.; Abdel-Raheem, S. A. A. Pyridine Derivatives as Insecticides. Part 1: Synthesis and Toxicity of Some Pyridine Derivatives Against Cowpea Aphid, Aphis craccivora Koch (Homoptera: Aphididae). *J. Agric. Food Chem.*, **2014**, *62*, 9982–9986.

(2) Eicher, T; Hauptmann, S. The Chemistry of Heterocycles: Structures, Reactions, Synthesis and Applications, 2nd ed.; Wiley-VCH: Wienheim, **2003**. (b) Joule, J. A.; Mills, K. *Heterocyclic Chemistry*, 4th ed.; Blackwell: Malden, MA, **2000**.

(3) (a) Hill, M. D. Recent Strategies for the Synthesis of Pyridine Derivatives. *Chem. Eur. J.* **2010**, *16*, 12052–12062. (b) Boger, D. L. Diels-Alder reactions of heterocyclic aza dienes. Scope and applications. *Chem. Rev.* **1986**, *86*, 781–793. (c) Kröhnke, F. The Specific Synthesis of Pyridines and Oligopyridines. *Synthesis* **1975**, 1–24.

(4) Schäfer, P.; Palacin, V.; Sidera, M.; Fletcher, S. P. Asymmetric Suzuki-Miyaura coupling of heterocycles via Rhodium-catalysed allylic arylation of racemates. *Nat Commun.* **2017**, *8*, 15762. (b) Dick, G. R.; Woerly, E. M.; Burke, M. D. A General Solution for the 2-Pyridyl Problem. *Angew. Chem. Int. Ed.* **2012**, *51*, 2667–2672. (c) Billingsley, K. L.; Anderson, K. W.; Buchwald, S. L. A Highly Active Catalyst for Suzuki-Miyaura Cross-Coupling Reactions of Heteroaryl Compounds. *Angew. Chem. Int. Ed.,* **2006**, *45,* 3484–3488.

(5)(a) Bull, J. A.; Mousseau, J. J.; Pelletier, G.; Charette, A. B. Synthesis of Pyridine and Dihydropyridine Derivatives by Regio- and Stereoselective Addition to N-Activated Pyridines. *Chem. Rev.* **2012**, 112, 2642–2713. (b) Nakao, Y.; Kanyiva, K. S.; Hiyama, T. A Strategy for C−H Activation of Pyridines: Direct C-2 Selective Alkenylation of Pyridines by Nickel/Lewis Acid Catalysis. *J. Am. Chem. Soc.* **2008**, *130*, 2448–2449. (c) Cho, S. H.; Hwang, S. J.; Chang. S. Palladium-Catalyzed C−H Functionalization of Pyridine N-Oxides: Highly Selective Alkenylation and Direct Arylation with Unactivated Arenes. *J. Am. Chem. Soc.* **2008**, *130*, 9254–9256.

(6) Bunnett, J. F.; Zahler, R. E. Aromatic Nucleophilic Substitution Reactions. *Chem. Rev.* **1951**, *49*, 273–412.

(7) Yan. M.; Lo, J. C.; Edwards, J. T.; Baran. P. S. Radicals: Reactive Intermediates with Translational Potential. *J. Am. Chem. Soc.* **2016**, *138*, 12692–12714.

(8) Punta, C.; Minisci, F. Minisci reaction: a Friedel-Crafts type process with opposite reactivity and selectivity. Selective homolytic alkylation, acylation, carboxylation and carbamoylation of heterocyclic aromatic bases. *Trends Het. Chem.* **2008**, *13*, 1–68.

(9) (a) Duncton, M. A. J. Minisci reactions: Versatile CH-functionalizations for medicinal chemists. *Med. Chem. Commun.* **2011**, *2*, 1135–1161. (b) Minisci, F.; Citterio, A.; Giordano, C. Electron-transfer processes: peroxydisulfate, a useful and versatile reagent in organic chemistry. *Acc. Chem. Res.* **1983**, *16*, 27–32.

(10) (a) Aycock, R. A.; Wang, H.; Jui, N. T. A mild catalytic system for radical conjugate addition of nitrogen heterocycles. *Chem. Sci.* **2017**, *8*, 3121–3125. (b) Aycock, R. A.; Vogt, D. B.; Jui, N. T. A practical and scalable system for heteroaryl amino acid synthesis. *Chem. Sci.* **2017**, *8*, 7998–8003.

(11) Boyington, A. J.; Riu, M.-L.; Jui, N. T. Anti-Markovnikov Hydroarylation of Unactivated Olefins via Pyridyl Radical Intermediates. *J. Am. Chem. Soc.* **2017**, *139*, 6582–6585.

(12) Heinrich, M. R. Intermolecular Olefin Functionalisation Involving Aryl Radicals Generated from Arenediazonium Salts. *Chem. Eur. J.* **2009**, *15*, 820–833.

(13) Shaw, M. H.; Twilton. J.; MacMillan, D. W. C. Photoredox Catalysis in Organic Chemistry. *J. Org. Chem.* **2016**, *81*, 6898–6926.

(14) Ma, X.; Herzon, S. B. Intermolecular Hydropyridylation of Unactivated Alkenes. *J. Am. Chem. Soc.* **2016**, *138*, 8718–8721. (b) Ma, X.; Dang, H.; Rose, J. A.; Rablen, P.; Herzon, S. B. Hydroheteroarylation of Unactivated Alkenes Using N-Methoxyheteroarenium Salts. *J. Am. Chem. Soc.* **2017**, *139*, 5998–6007.

(15) (a) Green, S. A.; Matos, J. L. M.; Yagi, A.; Shenvi, R. A. Branch-Selective Hydroarylation: Iodoarene–Olefin Cross-Coupling. *J. Am. Chem. Soc.* **2016**, *138*, 12779–12782. (b) Green, S. A.; Vásquez-Céspedes, S.; Shenvi, R. A. Iron–Nickel Dual-Catalysis: A New Engine for Olefin Functionalization and the Formation of Quaternary Centers. *J. Am. Chem. Soc.*, Article ASAP DOI: 10.1021/jacs.8b05868.

(16) Roberts, B. P. Polarity-reversal catalysis of hydrogen-atom abstraction reactions: concepts and applications in organic chemistry. *Chem. Soc. Rev.* **1999**, *28*, 25–35.

(17) Recupero, F.; Punta, C. Free Radical Functionalization of Organic Compounds Catalyzed by N-Hydroxyphthalimide. *Chem. Rev.* **2007**, *107*, 3800–3842.

(18) Cooper, J. C.; Luo, C.; Kameyama, R.; Van Humbeck, J. F. Combined Iron/Hydroxytriazole Dual Catalytic System for Site Selective Oxidation Adjacent to Azaheterocycles. *J. Am. Chem. Soc.* **2018**, *140*, 1243–1246.

(19) Denes, F.; Pichowicz, M.; Povie, G.; Renaud, P. Thiyl Radicals in Organic Synthesis. *Chem. Rev.* **2014**, *114*, 2587–2693.

(20) (a) Debuigne, A.; Caille, J.-R.; Jérôme, R. Highly Efficient Cobalt-Mediated Radical Polymerization of Vinyl Acetate. *Angew. Chem. Int. Ed.* **2005**, *44*, 1101–1104. (b) Percec, V.; Popov, A. V.; Ramirez-Castillo, E.; Monteiro, M.; Barboiu, B.; Weichold, O.; Asandei, A. D.; Mitchell, C. M. Aqueous Room Temperature Metal-Catalyzed Living Radical Polymerization of Vinyl Chloride. *J. Am. Chem. Soc.* **2002**, *124*, 4940–4941.

(21) Over half of the reports for vinyl pyridine synthesis from halopyridines come from stannanes. The remaining examples are mostly boron reagents–Scifinder 2018. For an example of Stille coupling to form vinyl pyridines see: Nuñez, A.; Abarca, B.; Cuadro, A. M.; Alvarez-Builla, J.; Vaquero, J. J. Ring-Closing Metathesis Reactions on Azinium Salts: Straightforward Access to Quinolizinium Cations and Their Dihydro Derivatives. *J. Org. Chem.* **2009**, *74*, 4166–4176.

(22) Nielsen, M. K.; Ugaz, C. R.; Li, W.; Doyle, A. G. PyFluor: A Low-Cost, Stable, and Selective Deoxyfluorination Reagent *J. Am. Chem. Soc.* **2015**, *137*, 9571−9574.

(23) Noble, A.; Mega, R. S.; Pflästerer, D.; Myers, E. L.; Aggarwal, V. K. Visible-Light-Mediated Decarboxylative Radical Additions to Vinyl Boronic Esters: Rapid Access to γ-Amino Boronic Esters. *Angew. Chem. Int. Ed.* **2018**, *57*, 2155–2159.

(24) The reactivity of α-oxy and α-amino radicals is well studied. For examples of the reactivity of α-oxy radicals see: (a) Tang, X.; Studer, A. Sodium-Ketyl Radical Anions by Reverse Pinacol Reaction and Their Coupling with Iodoarenes. *Org. Lett.* **2016**, *18*, 4448–4450. (b) Zhang, W.-C.; Li, C.-J. Magnesium-Mediated Carbon−Carbon Bond Formation in Aqueous Media: Barbier−Grignard Allylation and

Pinacol Coupling of Aldehydes. *J. Org. Chem.* **1999**, *64*, 3230–3236. (c) Jeffrey, J. L.; Terrett, J. A.; MacMillan, D. W. C. O–H hydrogen bonding promotes H-atom transfer from α C–H bonds for C-alkylation of alcohols. *Science*, **2015**, *349*, 1532–1536. For examples of the reactivity of α-amino radicals see: (d) Shaw, M. H.; Shurtleff, V. W.; Terrett, J. A.; Cuthbertson, J. D.; MacMillan, D. W. C. Native functionality in triple catalytic cross-coupling: sp3 C–H bonds as latent nucleophiles. *Science*, **2016**, *352*, 1304–1308. (e) Espelt, L. R.; McPherson, I. S.; Wiensch, E. M.; Yoon T. P. Enantioselective Conjugate Additions of α-Amino Radicals via Cooperative Photoredox and Lewis Acid Catalysis. *J. Am. Chem. Soc.* **2015**, *137*, 2452–2455. For a recent example of degradation of α-halo radicals to aldehydes see: (f) Ma, X.; Herzon, S. B. Synthesis of Ketones and Esters from Heteroatom-Functionalized Alkenes by Cobalt-Mediated Hydrogen Atom Transfer. *J. Org. Chem.* **2016**, *81*, 8673−8695.

(25) Carrolla, M. P.; Guiry, P. J. P,N ligands in asymmetric catalysis. *Chem. Soc. Rev.* **2014**, *43*, 819–833.

(26) Primary alcohols can be oxidized under Heck conditions. For an example see: HyunKim, B.; Lee, J. G.; Yim, T.; Kim, H.-J.; Lee, H. Y.; Kim Y. G. Highly efficient two-step selective synthesis of 2,6-dimethylnaphthalene. *Tetrahedron Lett.* **2006**, *47*, 7727–7730.

(27) Sohda, T.; Ikeda, H.; Megura, K. Studies on Antidiabetic Agents. XII. Synthesis and Activity of the Metabolites of (±)-5-[p-[2-(5-Ethyl-2-pyridyl)ethoxy]benzyl]-2, 4-thiazolidinedione (Pioglitazone). *Chem. Pharm. Bull.* **1995**, *43*, 2168–2172.

(28) Beeler, A. B.; Schaus, S. E.; Porco Jr, J. A. Chemical library synthesis using convergent approaches. *Curr. Opin. Chem. Biol.* **2005**, *9*, 277–284.

(29) Tucker, J. W.; Zhang, Y.; Jamison, T. F.; Stephenson, C. R. J. Visible-Light Photoredox Catalysis in Flow. *Angew. Chem. Int. Ed.* **2012**, 5*1*, 4144–4147.

(30) (a) Plutschack, M. B.; Pieber, B.; Gilmore, K.; Seeberger, P. H. The Hitchhiker's Guide to Flow Chemistry. *Chem. Rev.* **2017**, *117*, 11796–11893. (b) Lima, F.; Kabeshov, M. A.; Tran, D. N.; Battilocchio, C.; Sedelmeier, J.; Sedelmeier, G.; Schenkel, B.; Ley, S. V. Visible Light Activation of Boronic Esters Enables Efficient Photoredox C(sp2)–C(sp3) Cross-Couplings in Flow. *Angew. Chem. Int. Ed.* **2016**, *55,* 14085–14089.

(31) (a) Beatty, J. W.; Douglas J. J.; Miller R.; McAtee, R. C.; Cole, K. P.; Stephenson, C. R. J. Photochemical Perfluoroalkylation with Pyridine N-Oxides: Mechanistic Insights and Performance on a Kilogram Scale. *Chem* **2016**, *1*, 456–472. (b) Caron, A.; Hernandez-Perez, A. C.; Collins, S. K. Synthesis of a Carprofen Analogue Using a Continuous Flow UV-Reactor. *Org. Process Res. Dev.* **2014**, *18*, 1571–1574. (c) Šterk, D.; Juki č , M.; Č asar, Z. Application of Flow Photochemical Bromination in the Synthesis of a 5-Bromomethylpyrimidine Precursor of Rosuvastatin: Improvement of Productivity and Product Purity. *Org. Process Res. Dev.* **2013**, *17*, 145–151. (d) Lévesque, F.; Seeberger P. H. Continuous-flow synthesis of the anti-malaria drug artemisinin. *Angew. Chem. Int. Ed.* **2012**, *51*, 1706–1709.

(32) Rono, L. J.; Yayla, H. G.; Wang, D. Y.; Armstrong, M. F.; Knowles, R. R. Enantioselective Photoredox Catalysis Enabled by Proton-Coupled Electron Transfer: Development of an Asymmetric Aza-Pinacol Cyclization. *J. Am. Chem. Soc.* **2013**, *135*, 17735–17738.

(33) Bégué, J.-P.; Bonnet-Delpon, D.; Crousse, B. Fluorinated Alcohols: A New Medium for Selective and Clean Reaction. *Synlett*, **2004**, *1*, 18–29.

(34) Holubek, J.; Volke, J. Polarography of heterocyclic aromatic compounds. XIII. Polarographic fission of carbon-halogen bonds in monohalogenopyridines. *Collect. Czech. Chem. Commun.* **1962**, *27*, 680–692.

(35) (a) Enemærke, R. J.; Christensen, T. B.; Jensen, H.; Daasbjerg, K. Application of a new kinetic method in the investigation of cleavage reactions of haloaromatic radical anions. *J. Chem. Soc., Perkin Trans. 2* **2001**, 1620–1630. (b) Andrieux, C. P.; Blocman, C.; Dumas-Bouchiat, J.-M.; Saveant, J.-M. Heterogeneous and homogeneous electron transfers to aromatic halides. An electrochemical redox catalysis study in the halobenzene and halopyridine series. *J. Am. Chem. Soc.* **1979**, *101*, 3431–3441.

(36) (a) Tarantino, K. T.; Liu, P.; Knowles, R. R. Catalytic Ketyl-Olefin Cyclizations Enabled by Proton-Coupled Electron Transfer. *J. Am. Chem. Soc.* **2013**, *135*, 10022–10025. (b) Weinberg, D. R.; Gagliardi, C. J.; Hull, J. F.; Murphy, C. F.; Kent, C. A.; Westlake, B. C.; Paul, A.; Ess, D. H.; McCafferty, D. G.; Meyer, T. J. Proton-Coupled Electron Transfer. *Chem. Rev.* **2012**, *112*, 4016–4093.

(37) (a) Yan, Y.; Zeitler, E. L.; Gu, J.; Hu, Y.; Bocarsly, A. B. Electrochemistry of Aqueous Pyridinium: Exploration of a Key Aspect of Electrocatalytic Reduction of CO2 to Methanol. *J. Am. Chem. Soc.* **2013**, *135*, 14020–14023. (b) Keith, J. A.; Carter, E. A. Theoretical Insights into Pyridinium-Based Photoelectrocatalytic Reduction of CO_2. *J. Am. Chem. Soc.* **2012**, *134*, 7580–7583.

(38) DFT calculations were also performed using different levels of theory with different solvation parameter, giving a range of values for pyridine reduction potentials, see SI for full details.

(39) Joerg, S.; Drago, R. S.; Adams, J. Donor–acceptor and polarity parameters for hydrogen bonding solvents. *J. Chem. Soc., Perkin Trans. 2*, **1997**, 2431–2438.

(40) Krishnan, R.; Fillingim, T. G.; Lee, J.; Robinson, G. W. Solvent structural effects on proton dissociation. *J. Am. Chem. Soc.* **1990**, *112*, 1353–1357.

(41) (a) Arora, A.; Teegardin, K.; Weaver, J. D. Reductive Alkylation of 2-Bromoazoles via Photoinduced Electron Transfer: A Versatile Strategy to Csp2–Csp3 Coupled Products. *Org. Lett.* **2015**, *17*, 3722–3725. (b) Singh, A.; Arora, A.; Weaver, J. D. Photoredox-Mediated C–H Functionalization and Coupling of Tertiary Aliphatic Amines with 2-Chloroazoles. *Org. Lett.* **2013**, *15*, 5390–5393. (c) Arora, A.; Weaver, J. D. Photocatalytic Generation of 2-Azolyl Radicals: Intermediates for the Azolylation of Arenes and Heteroarenes via C–H Functionalization. *Org. Lett.* **2016**, *18*, 3996–3999.

(42) Andrieux, C. P.; Robert, M.; Saveant, J.-M. Role of Environmental Factors in the Dynamics of Intramolecular Dissociative Electron Transfer. Effect of Solvation and Ion-Pairing on Cleavage Rates of Anion Radicals. *J. Am. Chem. Soc.* **1995**, *117*, 9340–9346.

(43) Geise, B. Formation of CC Bonds by Addition of Free Radicals to Alkenes. *Angew. Chem. Int. Ed.* **1983**, *22*, 753–764.

(44) Giese, B.; González-Gómez, J. A.; Witzel, T. The Scope of Radical CC-Coupling by the "Tin Method". *Angew. Chem. Int. Ed.* **1984**, *23*, 69–70.

(45) Yin, Y.; Dai, Y.; Jia, H.; Li, J.; Bu. L.; Qiao, B.; Zhao, X.; Jiang, Z. Conjugate Addition–Enantioselective Protonation of N-Aryl Glycines to α-Branched 2-Vinylazaarenes via Cooperative Photoredox and Asymmetric Catalysis. *J. Am. Chem. Soc.* **2018**, 140, 6083–6087.

(46) Chernyak, N; Buchwald, S. L. Continuous-Flow Synthesis of Monoarylated Acetaldehydes Using Aryldiazonium Salts. *J. Am. Chem. Soc.* **2012**, *134*, 12466–12469.

(47) Campbell, J. M.; Xu, H.-C.; Moeller, K. D. Investigating the Reactivity of Radical Cations: Experimental and Computational Insights into the Reactions of Radical Cations with Alcohol and p-Toluene Sulfonamide Nucleophiles. *J. Am. Chem. Soc.* **2012**, *134*, 18338–18344.

(48) Horner, J. H.; Taxil, E.; Newcomb, M. Laser Flash Photolysis Kinetic Studies of Enol Ether Radical Cations. Rate Constants for Heterolysis of α -Methoxy- β -phosphatoxyalkyl Radicals and for Cyclizations of Enol Ether Radical Cations. *J. Am. Chem. Soc.* **2002**, *124*, 5402–5410.

(49) Le, C.; Wismer, M. K.; Shi, Z.-C.; Zhang, R.; Conway, D. V.; Li, G.; Vachal, P; Davies, I. W.; MacMillan, D. W. C. A General Small-Scale Reactor To Enable Standardization and Acceleration of Photocatalytic Reactions. *ACS Cent. Sci.* **2017**, *3*, 647–653.

(50) Cismesia, M. A.; Yoon, T. P. Characterizing chain processes in visible light photoredox catalysis. *Chem. Sci.* **2015**, *6*, 5426–5434.

(51) Huang, W.; Cheng, X. Hantzsch Esters as Multifunctional Reagents in Visible-Light Photoredox Catalysis. *Synlett*, **2017**, *28*, 148–158.

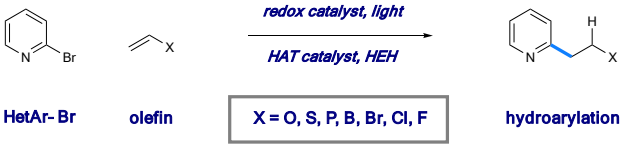
redox catalyst, light
HAT catalyst, HEH
N
Br
X
H
N
X
HetAr- Br
olefin
X = O, S, P, B, Br, Cl, F
hydroarylation